Catalysis Today 144 (2009) 278–284

Contents lists available at ScienceDirect

Catalysis Today

journal homepage: www.elsevier.com/locate/cattod

Aerogel VO_x/MgO catalysts for oxidative dehydrogenation of propane

Ilya V. Mishakov [a,*], Aleksey A. Vedyagin [a], Alexander F. Bedilo [a], Vladimir I. Zaikovskii [a], Kenneth J. Klabunde [b]

[a] Boreskov Institute of Catalysis, Novosibirsk 630090, Russia
[b] Department of Chemistry, Kansas State University, Manhattan, Kansas 66506, USA

ARTICLE INFO

Article history:
Available online 12 February 2009

Keywords:
Nanoparticles
Aerogels
Vanadium
Magnesium oxide
Oxidative dehydrogenation
Propane
Propene
Iodine

ABSTRACT

VO_x/MgO aerogel catalysts were synthesized using three different preparation methods: by mixing the aerogel MgO support with dry ammonium vanadate, by vanadium deposition from a precursor solution in toluene, and by hydrolysis of a mixture of vanadium and magnesium alkoxides followed by co-gelation and supercritical drying. The latter aerogel technique allowed us to synthesize mixed vanadium–magnesium hydroxides with the surface areas exceeding 1300 m^2/g. The synthesized catalysts were studied by a number of physicochemical methods (XRD, Raman spectroscopy, XANES and TEM). A common feature of all synthesized samples is the lack of V_2O_5 phase. In all cases vanadium was found to be a part of a surface mixed V–Mg oxide (magnesium vanadate), its structure depending on the synthesis method. The VO_x/MgO mixed aerogel sample had the highest surface area 340 m^2/g, showed higher catalytic activity and selectivity in oxidative dehydrogenation of propane compared to the catalysts prepared by impregnation and dry mixing. The addition of iodine vapor to the feed in 0.1–0.25 vol.% concentrations was found to increase to propylene yield by 40–70%.

1. Introduction

With increasing oil prices, an alternative process for the production of lower alkenes is economically reasonable. Oxidative dehydrogenation (ODH), e.g., of propane, is an attractive reaction route instead of steam cracking of naphtha or catalytic cracking/dehydrogenation [1,2]. This alternative process is energetically favorable due to lower reaction temperatures and enhanced catalyst lifetime thanks to prevention of the coke deposition. Furthermore, it is neither equilibrium-limited nor endothermic. Therefore, it has important advantages compared to the established processes. Due to the increasing world demand for propene, the ODH reaction is a great challenge for catalysis research and development, and growing attention has been focused on this topic in the past decade.

As pointed out by Brazdil [3]: "The direct conversion of ethane and propane to commodity chemical intermediates has the potential to radically transform the chemical industry. The effectiveness of the catalyst, that is the activity for alkane conversion and the selectivity to desired products, will ultimately determine the economic attractiveness of an alkane-based chemical process." However, in the case of alkenes produced from alkanes, the lower cost of the feedstock is not a real incentive, since current commercial technologies for olefin production already use fuel-grade feedstocks. In this case, conversely, the improved energy efficiency (ODH is exothermal, while dehydrogenation and cracking are endothermal), and process simplicity are effective incentives [4].

A considerable amount of work has been devoted to the development of catalysts with good selectivity to olefins in the oxidative dehydrogenation of paraffins. V/MgO was found to be one of the best catalytic systems in terms of activity and performance stability [5–9]. The reaction is believed to follow a Mars–van Krevelen reaction mechanism [10–16], in which adsorbed propane reacts with lattice oxygen and the reduced metal oxide reacts with adsorbed dissociated O_2 [17].

Despite good activity for the ODH of alkanes to their corresponding alkenes, non-selective combustion pathways limit the alkene selectivities, especially at high conversions [6,18–22]. Particularly for oxidative dehydrogenation of propane to propene, it has been well established that limited propene selectivity at higher propane conversions is related to propene adsorption on acid sites and their subsequent combustion to carbon oxides [19,23–24]. Thus, new efficient catalytic systems that would allow for effective propene production with high selectivity at higher propane conversions are highly desirable.

Nanocrystalline metal oxides prepared by a modified aerogel procedure developed by Klabunde and co-workers at KSU are known to have high surface areas, small crystallite sizes, unusual morphology, and enhanced adsorption properties in comparison with conventionally prepared materials [25–29]. Such materials

* Corresponding author. Tel.: +7 383 3269406.
E-mail address: mishakov@catalysis.ru (I.V. Mishakov).

0920-5861/$ – see front matter © 2009 Elsevier B.V. All rights reserved.
doi:10.1016/j.cattod.2009.01.018

have been successfully applied for destructive adsorption of various harmful organic substances. Moreover, their properties make them very good candidates for various applications as catalysts and catalyst supports [30–32]. Vanadia-doped MgO catalysts prepared by impregnating aerogel-prepared (AP) MgO with solutions of various vanadium precursors have been shown to be active catalysts for oxidative dehydrogenation of butane and propane [33–35].

In the current publication we report a new method for synthesis of VO_x/MgO mixed aerogels by hydrolysis of a mixture of vanadium and magnesium alkoxides followed by co-gelation and supercritical drying. The resulting materials were characterized by physical methods and studied in catalytic oxidative dehydrogenation of propane. Their properties were compared with those of VO_x/MgO catalysts prepared using other techniques for vanadia deposition on MgO aerogel supports. We also studied the effect of iodine on the performance of the VO_x/MgO catalysts in propane ODH. Earlier we showed that iodine addition significantly improves the activity and selectivity of VO_x/MgO catalyst in oxidative dehydrogenation of butane to butadiene [34].

2. Experimental

2.1. Reagents and materials

Three different methods were used for synthesis of vanadium catalysts supported on AP-MgO: mixing the aerogel MgO support with dry ammonium vanadate; vanadium deposition from a vanadium acetylacetonate solution in toluene; and hydrolysis of a mixture of vanadium and magnesium alkoxides followed by co-gelation and supercritical drying.

Magnesium methoxide was prepared by dissolving Mg metal ribbon (Fisher) in methanol. For synthesis of aerogel 10% [VO_x/MgO]-AP catalysts, 17 ml of a 1 M $Mg(OCH_3)_2$ solution in methanol was mixed with 79 ml toluene in a Schlenk flask. Then, vanadium oxytriisopropoxide (Aldrich) was added to the solution. The solution was further homogenized by stirring with a magnetic stir bar for 10 min. Then, 2.5 ml distilled deionized water used for hydrolysis was added dropwise to the solution. The mixture was allowed to stir overnight prior to being subjected to supercritical drying.

The high temperature supercritical drying of the gels was performed in a standard 1 l autoclave (Parr). The autoclave temperature was slowly increased to 265 °C at a rate of 1 °C per minute and maintained at that temperature for 10 min. After completion of the procedure, the pressure was quickly released by venting of solvent vapor. The sample was flushed with nitrogen for 10 min and allowed to cool down in nitrogen. Then, V–Mg hydroxide obtained after supercritical drying was dehydrated by heat treatment under vacuum for 12 h with the temperature gradually increased in small steps to 550 °C. Finally the sample was calcined in a muffle furnace in air at 600 °C for 2 h.

10%VO_x/MgO-AP sample with vanadyl acetylacetonate (Aldrich, 99%) used as a precursor was prepared by impregnation. MgO-AP (635 m^2/g) was then added with stirring to the $V(acac)_3$ solution in toluene, and stirring was continued under argon for 2–20 h. The sample was then filtered in a Buchner funnel attached to a water aspirator to remove the solvent. The resulting material was dried at 200 °C for 1 h and then calcined at 550 °C for 2 h in air.

The "dry" method used for synthesis of 10%VO_x/MgO-AP catalysts started with mixing the calculated amounts of NH_4VO_3 and AP-MgO. Then, the mixture was calcined in air at 600 °C for 4 h. At such temperatures NH_4VO_3 melts and interacts with the surface of the support. Such technique makes it possible to achieve relatively uniform distribution of the active component without using a solvent that could deteriorate the texture of the aerogel support.

2.2. Kinetic experiments

The performance of different catalysts in iodine-mediated oxidative dehydrogenation was studied in a 10 cm^3 quartz flow reactor. The reactor was placed inside an electrical furnace. The reaction was carried out in temperature range of 400–600 °C. The catalyst loadings were varied between 0.01 and 0.2 g. The feed flow rate was 2.5 l/h. The catalysts were diluted with quartz powder to prevent removal of the oxide particles by the gas flow. The feed composition (vol.%) was 90% He: 5% C_3H_8: 5% O_2.

The iodine concentration in the feed was varied between 0 and 0.25 vol.%. The feed was saturated with iodine in a bubbler maintained at certain temperature (ambient or 50 °C). The iodine concentration in the feed at room temperature was measured to be about 0.1 vol.%. The gas line between the bubbler and the reactor was heated to prevent iodine condensation on the walls.

The exit gases after the reactor were analyzed by gas chromatography using a GOW MAC 580 chromatograph with a TCD detector and Chromosorb CP-AW and Molecular Sieve columns.

2.3. Characterization of samples

Textural characterization of the samples was performed on a NOVA 1200 gas sorption analyzer (Quantachrome Corp.). Prior to the analysis, the samples were outgassed at 150 °C for 1 h. Seven point BET surface areas, total pore volumes, and average pore diameters were calculated from nitrogen adsorption isotherms.

X-ray powder diffraction experiments were conducted on a Scintag-XDS-2000 spectrometer with Cu Kα radiation. Scans were made in the 2θ range 20–80° with 1° per minute scanning rate.

Raman spectra were collected using a Nicolet Nexus 670 FTIR spectrometer with an FT-Raman attachment. The laser energy was 0.4 W at the wavelength of 1064 nm. The spectra were recorded using 1024 scans at 4 cm^{-1} resolution.

The vanadium K-edges for all samples were obtained at the EXAFS Station of Siberian Synchrotron Radiation Center. The storage ring VEPP-3 with electron beam energy of 2 GeV and an average stored current of 80 mA was used as the radiation source. The X-ray energy was monitored with a channel cut Si 1 1 1 monochromator. All the spectra were recorded under transmission mode using two ionization chambers as detectors. For the XANES measurements, the samples were prepared as pellets with a 0.5 absorption jump at the absorption edges.

Transmission electron microscopic (TEM) images were obtained with a JEM-100C (JEOL, Japan) transmission electron microscope at the resolution of 0.30 nm. A sample was crushed in ethanol slurry, and the resulting solution was dispersed on holey-carbon films mounted on copper grids.

3. Results and discussion

3.1. Synthesis of the catalysts

Information on the synthesis of 10%VO_x/MgO (calculated as V_2O_5) samples prepared by different methods and their surface areas is summarized in Table 1. All the catalysts used in this study either had vanadium deposited on the aerogel AP-MgO support, which was studied in detail earlier [25–35], or were prepared as mixed VO_x/MgO aerogels. The final heat treatment conditions were the same for all samples – calcination in a muffle furnace at 600 °C for 2 h. The surface area of the sample prepared by impregnation of the AP-MgO support (S.A. = 635 m^2/g) with a $VO(acac)_3$ solution in toluene (samples VO_x/MgO-AP(imp-2) and VO_x/MgO-AP(imp-20)) was about 160 m^2/g and did not depend on the deposition time. The surface area of the sample prepared by mechanical mixing (VO_x/MgO-AP(MM)) was somewhat higher, 215 m^2/g.

Table 1
Different methods used for synthesis of 10% VO_x/MgO-AP samples.

	Sample	Synthesis method	Synthesis stages	S.A. of AP-MgO support (m^2/g)	S.A. (m^2/g)
1	VO_x/MgO-AP(imp-2)	Impregnation with $VO(acac)_3$, 2 h	Drying at 200 °C (1 h) Calcination at 600 °C (2 h)	635	150
2	VO_x/MgO-AP(imp-20)	Impregnation with $VO(acac)_3$, 20 h	Drying at 200 °C (1 h) Calcination at 600 °C (2 h)	635	170
3	VO_x/MgO-AP(MM)	Mechanical mixing of AP-MgO with NH_4VO_3	Calcination at 600 °C (2 h)	500	215
4	[VO_x/MgO]-AP	Hydrolysis of $Mg(OCH_3)_2$ + $VO(O^iC_3H_7)_3$ solution	Autoclave drying at 265 °C, 55 bar (4 h) Evacuation at 550 °C Calcination at 600 °C (2 h)	N/A	340

The highest surface area was obtained for the mixed aerogel sample [VO_x/MgO]-AP prepared by hydrolysis of a mixed $Mg(OCH_3)_2$ and $VO(O^iC_3H_7)_3$ solution in a toluene-methanol mixture followed by co-gelation and supercritical drying. After drying in the autoclave, the obtained V–Mg hydroxide aerogel was heat treated in vacuum followed by calcination in air under standard conditions. The surface area of this sample was as high as 340 m^2/g. This is 1.5–2 times higher than the surface areas of the samples prepared by the "dry" method and by impregnation.

Table 2 shows how the surface area of the [VO_x/MgO]-AP sample changes at different preparation stages. The V–Mg hydroxide aerogel prepared after removing the solvent under supercritical conditions has exceptionally high surface area, 1320 m^2/g. Note that its surface area is higher than that of the aerogel magnesium hydroxide (AP-$Mg(OH)_2$). The highest surface area obtained for the latter was about 1100 m^2/g [25].

After dehydration under vacuum with the temperature gradually increased to 550 °C, the surface area of the sample decreases by a factor of 2.5. Calcination in air at 600 °C further decreases the surface area by a factor of 1.5. Still, the surface area of the aerogel calcined at 600 °C equal to 340 m^2/g was ca. twice higher than that of the other VO_x/MgO catalysts studied by us as well as reported in the literature. Meanwhile, the surface area of nanocrystalline MgO aerogel usually does not decrease more than twice after the heat treatment compared to the initial AP-$Mg(OH)_2$. Thus, vanadium introduction into the structure of the MgO aerogel increases the initial surface area after the supercritical drying, but makes the samples more prone to sintering during the heat treatment.

3.2. XRD characterization

According to the XRD pattern of VO_x/MgO-AP(imp-20) sample prepared by impregnation, the vanadium-containing component exists in the form of traces of partially crystallized phases $Mg_3(VO_4)_2$ [36] and $Mg(VO_3)_2$ [37] (Fig. 1). It is important that these reflexes do not correspond to the V_2O_5 [38] phase (Fig. 1, diffraction pattern 3). The most intense line at about 37° (2θ) can be attributed to magnesium oxide MgO [39].

Nanocrystalline magnesium oxide was the only phase unambiguously identified for [VO_x/MgO]-AP mixed aerogel sample. The average MgO crystallite size was 5 nm. Meanwhile, the signal of the vanadium component was too wide to be attributed to any of the known vanadium-magnesium mixed oxides. Thus, XRD does not give sufficient information on the structure of supported vanadium in aerogel VO_x/MgO catalysts.

Table 2
Changes of the textural characteristics of aerogel 10%[VO_x/MgO]-AP sample after different synthesis stages.

	Synthesis stage	S_{BET} (m^2/g)	Average pore diameter (Å)
1	Autoclave drying (P = 55 bar, T = 265 °C)	1320	35
2	Dehydration in vacuum at 550 °C	500	40
3	Calcination in air at 600 °C	340	60

3.3. Raman spectroscopy

To gain additional information on the phase composition of VO_x/MgO samples we used Raman spectroscopy. Fig. 2 shows Raman spectra of the samples prepared by the aerogel ([VO_x/MgO]-AP] and impregnation (VO_x/MgO-AP(imp-20)) methods. Raman spectrum of commercial magnesium orthovanadate is shown for comparison. The analysis of the results suggests that magnesium orthovanadate $Mg_3(VO_4)_2$ (Raman band at 860 cm^{-1}) is the main vanadium phase in the sample prepared by impregnation. A weaker band at 950 cm^{-1} most likely corresponds to magnesium pyrovanadate $Mg_2V_2O_7$ [40,41]. This result agrees will the literature data on impregnated [VO_x/MgO]-AP catalysts [35]. It was shown that the active component in such samples consists of a mixture of magnesium ortho- and pyrovanadates, the fraction of the latter growing when the vanadium concentration increases.

In the case of the aerogel VO_x/MgO catalyst, the only wide band in the region of 700–850 cm^{-1} with a sharp maximum at 740 cm^{-1} is observed in Raman spectrum (Fig. 2, Sp. 3). Such spectrum cannot be attributed to any known magnesium vanadate phase. Thus, Raman spectroscopy also does not allow for reliable identification of the active component structure in aerogel VO_x/MgO samples.

3.4. XANES data

It is well known that the vanadium K-edge is very sensitive to the local symmetry of the vanadium site [42]. The XANES spectra

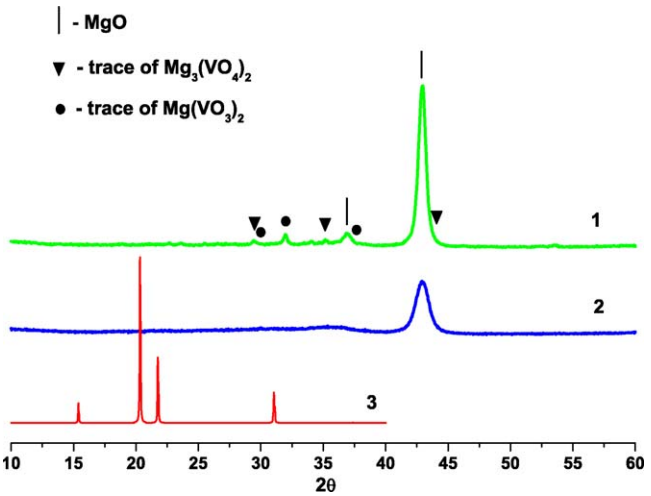

Fig. 1. XRD diffraction profiles for VO_x/MgO samples: (1) VO_x/MgO-AP(imp-20); (2) aerogel [VO_x/MgO]-AP; (3) V_2O_5 (given as a reference).

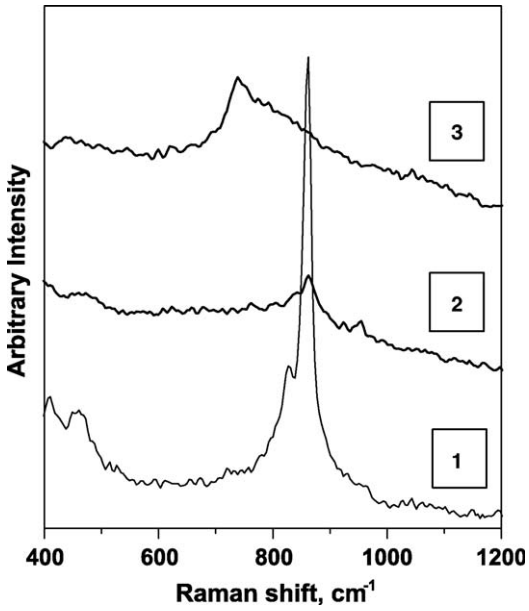

Fig. 2. Raman spectra of VO_x/MgO samples: (1) magnesium orthovanadate $Mg_3(VO_4)_2$; (2) VO_x/MgO-AP(imp-20); (3) aerogel [VO_x/MgO]-AP.

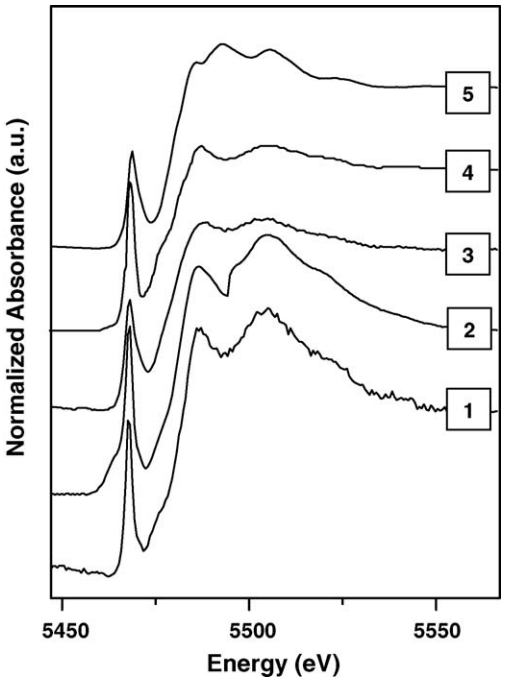

Fig. 3. XANES spectra at the vanadium K-edge: (1) [VO_x/MgO]-AP; (2) VO_x/MgO-AP(imp-2); (3) VO_x/MgO-AP(MM); (4) VO_x/MgO-AP (from [35]); (5) V_2O_5.

of all samples presented in Fig. 3 show a pre-edge peak, which is responsible for the formally forbidden 1s–3d electronic transition. However, it is partially allowed due to mixing of 3d and 4p orbitals and overlap of the vanadium 3d orbitals with the 2p orbitals of neighboring oxygen [43,44]. This transition does not occur in a regular octahedral symmetry having a center of inversion. The pre-edge absorption becomes dipole-allowed in part when the symmetry of the ligands is changed to tetrahedral [45]. Thus, the vanadium in all these samples is likely to have tetrahedral rather than octahedral oxygen environment.

The sharpness of the pre-edge peak depends on the spread of V–O distances [35,46]. A larger spread of the V–O distances gave broader pre-edge peaks in a series of tetrahedral vanadium compounds [43]. The peak widths at half-height are presented in Table 3. Comparison of the peak widths of [VO_x/MgO]-AP, VO_x/MgO-AP(imp-2) and VO_x/MgO-AP(MM) catalysts suggests that the spread of V–O distances is close to that in NH_4VO_3, which is characterized by the pre-edge peak width of 2.55 ± 0.2 eV [39].

The main edge region also called edge resonance is associated with the continuum and is due to Multiple Scattering resonances of photoelectrons [47]. The intensity and the shape of the edge region are affected by the symmetry of the four basal oxygen atoms surrounding the vanadium sites [44]. For the V_2O_5 there are three peaks in this region. The first peak at around 5486 eV and the third peak at around 5505 eV are common for vanadium compounds and supported vanadium catalysts [43,46]. The presence of the second peak at ca. 5492 eV indicates the existence of V_2O_5 crystallites on the sample. It can be clearly seen that there are no peaks at ca. 5492 eV in the spectra of all supported vanadium catalysts.

The spectra show differences in the intensity of the edge resonance of the catalysts prepared by the different methods. The shapes of the spectra for all samples are very similar to that of the reference spectrum of impregnated VO_x/MgO-AP sample (4), which was taken from ref. [35]. Based on the attribution of this reference spectrum, the surface phase in all our supported VO_x/MgO can be attributed to magnesium orthovanadate and/or magnesium pyrovanadate with the likely presence of non-crystalline surface vanadium compounds. The only exception was observed in the spectrum of VO_x/MgO-AP(imp-2), which had a shoulder at 5497 eV. The presence of this shoulder can be explained by the existence of an additional VO phase.

3.5. TEM characterization

High-resolution transmission electron microscopy (TEM) was used to determine the morphology and distribution of the active component in VO_x/MgO-AP samples synthesized by different methods. The structure of VO_x/MgO-AP(MM) catalyst prepared by the "dry" deposition method in shown in Fig. 4. The sample consists of disordered aggregates of thin MgO plates with typical dimensions: width ~50 nm, thickness ~7 nm. These plates are sometimes assembled in secondary grid-like particles about 1 μm in size. According to the EDX data presented in Table 4, vanadium is present only in trace amounts in both types of MgO particle aggregates. No particles of a vanadate phase were observed.

Table 3
Summary of XANES results for VO_x/MgO catalysts and reference materials.

Sample	Pre-edge peak position (eV)	Pre-edge peak width (eV)	Edge peaks position (eV)		
			First	Second	Third
[VO_x/MgO]-AP	5467.7	2.5	5486.6	–	5504.7
VO_x/MgO-AP(imp-2)	5468.1	2.5	5486.6	–	5504.9
VO_x/MgO-AP(MM)	5468.1	2.8	5487.6	–	5504.8
VO_x/MgO-AP[r5]	5468.4	2.3	5487.4	–	5504.7
V_2O_5	5468.7	3.7	5485.9	5492.9	5505.8

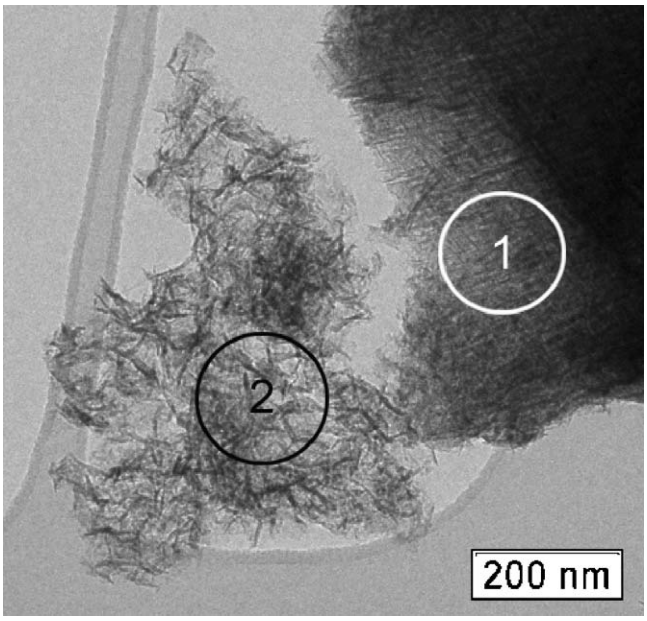

Fig. 4. TEM image of VO_x/MgO-AP(MM) catalyst prepared by mechanical mixing. Circled areas #1 and #2 were studied with EDX analysis.

The morphology of VO_x/MgO-AP(imp-20) catalyst prepared by impregnation is presented in Fig. 5. The dimensions of aggregated isometric MgO crystallites are somewhat larger than in the previous sample, about 10 nm. The vanadate phase in this sample mostly exists in the form of large particles with typical dimensions bigger than 200 nm. The active component distribution in this sample is not uniform, which is evidenced by the EDX spectra recorded from different parts of sample (Table 4).

A TEM image of aerogel [VO_x/MgO]-AP catalyst is shown in Fig. 6. This sample consists of isometric elongated nanocrystals ca. 5 nm in size. According to the EDX data (Table 4), the concentration of vanadium (related to magnesium) is 4.3–4.5 at.%, which corresponds to ca. 10 wt.% of V_2O_5 in MgO. Thus, the distribution of vanadium in aerogel [VO_x/MgO]-AP catalyst appears to be quite uniform and its concentration revealed by EDX analysis agrees well with the calculated one. No separate MgO nanocrystals were found in this sample.

Overall, it appears that unlike impregnation and mechanical mixing methods, the aerogel synthesis of VO_x/MgO catalysts allows one to obtain finely dispersed nanocrystalline samples with a uniform distribution of the active component throughout the sample.

Table 4
Chemical composition of VO_x/MgO samples prepared by different methods according to the EDX data.

	Sample	Atomic % by element	
		Mg	V
1	VO_x/MgO-AP(MM)		
	Area 1	99.8	0.2
	Area 2	99.8	0.2
2	VO_x/MgO-AP(imp-20)		
	Area 1	99.1	0.9
	Area 2	56.4	43.6
	Area 3	67.3	32.7
3	[VO_x/MgO]-AP		
	Area 1	95.5	4.5
	Area 2	95.7	4.3

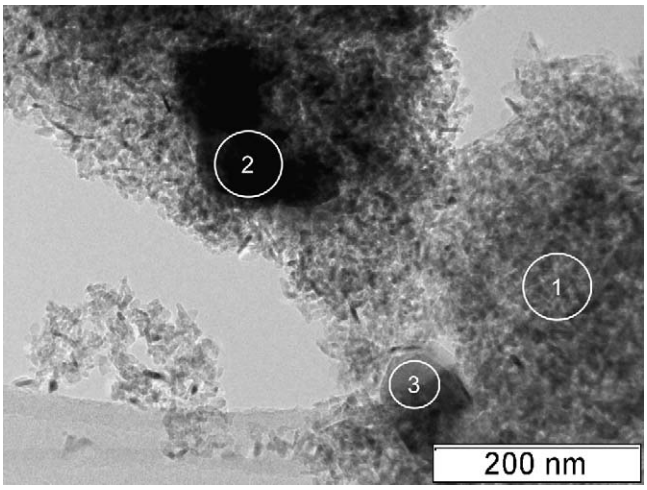

Fig. 5. TEM image of VO_x/MgO-AP(imp-20) catalyst prepared by impregnation. Circled areas #1, #2 and #3 were studied with EDX analysis.

3.6. Catalytic tests

Table 5 presents the results of catalytic tests of VO_x/MgO catalysts prepared by different methods in oxidative dehydrogenation of propane. The vanadium concentration in all samples was 10 wt.% (calculated as V_2O_5), the weight of all catalyst samples was 0.05 g. Thermal conversion of propane in an empty reactor begins only at 600 °C. Even at this temperature the propane conversion is only 3%, and propene selectivity is very low, 7%. The activity of the AP-MgO support (S.A. 635 m^2/g) is considerably higher, but its C_3H_6 selectivity is also unacceptably low, 10-12%. Vanadium deposition on AP-MgO by the "dry" method results in a significant increase of the selectivity to the desired product (70% at 500 °C). However, the activity of VO_x/MgO-AP(MM) catalyst prepared by this method is still lower than those of the catalysts prepared by impregnation and aerogel method.

VO_x/MgO-AP(imp-20) catalyst prepared by impregnation had high activity in propane ODH, but its selectivity to propylene did not exceed 35% even at low propane conversions (Table 5). Finally, [VO_x/MgO]-AP catalyst prepared by the novel aerogel method developed by us showed the best results among all samples tested in propane ODH. The propane conversion on this sample starts at lower temperature (425 °C). At low conversions ($X < 5\%$) the propylene selectivity is 70–80%. At higher conversions the selectivity

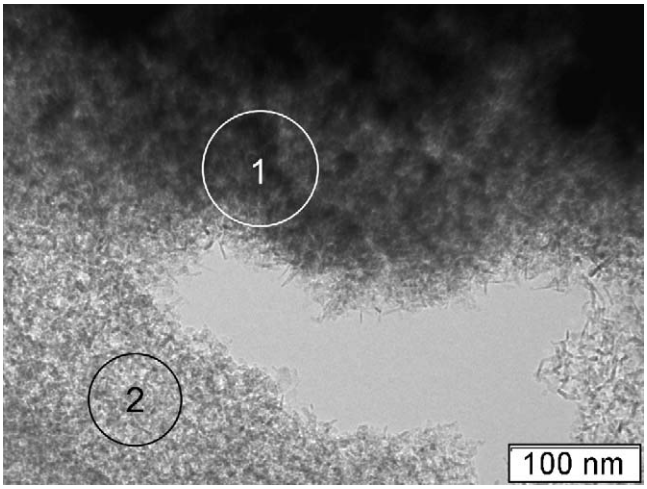

Fig. 6. TEM image of mixed aerogel [VO_x/MgO]-AP catalyst. Circled areas #1 and #2 were studied with EDX analysis.

Table 5
Activity and selectivity of 10% VO_x/MgO-AP catalysts prepared by different methods in oxidative dehydrogenation of propane.

	Catalyst	T (°C)	X (%)	S(C_3H_6) (%)	S(CO + CO_2) (%)	S(C_2) (%)
1	Empty reactor	550	0	–	–	–
		600	3	7	93	–
2	AP-MgO, S.A. = 635 m^2/g	450	0	–	–	–
		500	12	10	90	0
		550	24	11	89	0
		600	40	12	88	0
3	VO_x/MgO-AP(MM)	450	0	–	–	–
		500	2	70	30	0
		550	7.5	41	55	4
4	VO_x/MgO-AP(imp-20)	450	3	35	65	0
		500	8.5	33	67	0
		550	24	24	73	3
5	[VO_x/MgO]-AP	425	1.5	80	20	0
		450	4.5	69	31	0
		500	23	33	67	0
		550	30	28	70	2

to C_3H_6 decreased for all samples. This is a common feature for all catalysts in this reaction because propene formed in the desired reaction is also partially converted on surface acid sites to carbon oxides, thus, decreasing the selectivity.

A comparison diagram showing the catalyst productivity calculated as the propene yield ($g_{C3H6}/(g_{cat}\cdot h)$) achieved in one reaction cycle for 10% VO_x/MgO catalysts synthesized by three different methods is presented in Fig. 7. This diagram shows that the aerogel [VO_x/MgO]-AP sample has the best productivity in the whole studied temperature range. For example, at 500 °C the propylene yield over the aerogel catalyst was three times higher than that of the sample prepared by impregnation. It is important that this catalyst was both the most active at the same temperature and the most selective at any given conversion.

Thus, the aerogel method developed by us makes it possible to synthesize nanocrystalline VO_x/MgO catalysts with propene yield in oxidative dehydrogenation of propane significantly higher than those obtained for the samples synthesized by mechanical mixing ("dry" method) and impregnation. The previous studies showed that the catalysts prepared by impregnating AP-MgO with vanadia precursors performed better than VO_x/MgO catalysts prepared using conventional MgO supports [33,35], which are extensively studied in this reaction. Thus, it appears that the mixed aerogel method used in this study allows for synthesis of the most productive VO_x/MgO catalysts.

Here it is important to understand that according to the XANES data the nature of the vanadium component in the most active mixed aerogel catalysts is not too different from that observed in the other samples. In all the catalysts, vanadium atoms are surrounded by a tetragonal environment of oxygen atoms. Consequently, the observed differences in the activity should be attributed to higher dispersity and more uniform distribution of the active component achieved by the mixed aerogel synthesis of VO_x/MgO catalysts.

3.7. Promoting effect of iodine

We have earlier shown the promoting effect of iodine in oxidative dehydrogenation of butane to butadiene-1,3 over VO_x/MgO-AP catalyst prepared by impregnation [34]. Here we studied the effect of small amounts of iodine added to the feed on propane ODH over aerogel [VO_x/MgO]-AP catalyst (Fig. 8). The presence of iodine vapor in concentrations 0.1–0.25 vol.% led to a significant increase of the

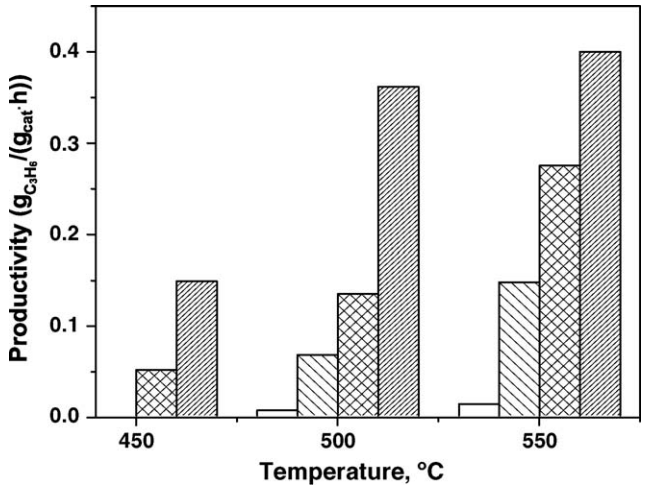

Fig. 7. Propene yield in propane ODH over AP-MgO and 10%VO_x/MgO prepared by different methods: □–AP-MgO; ▨–VO_x/MgO-AP(MM); ▩–VO_x/MgO-AP(imp-20; ▨–[VO_x/MgO]-AP.

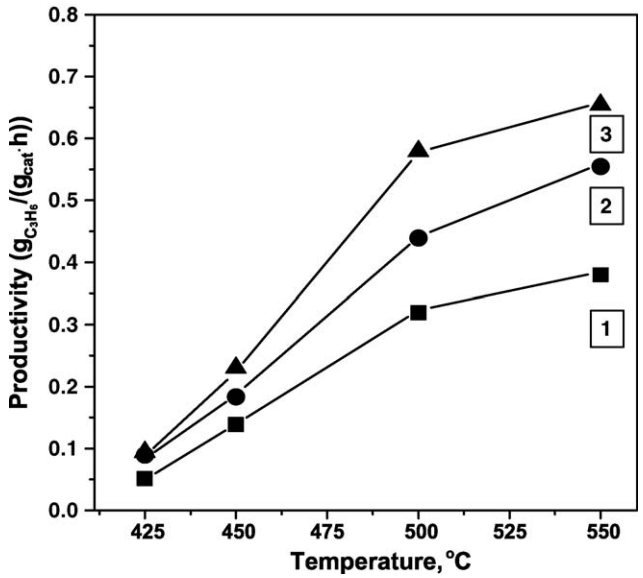

Fig. 8. Effect of small amounts of iodine added to the feed on propene yield in propane ODH over mixed aerogel [VO_x/MgO]-AP catalyst: (1) without I_2; (2) 0.1 vol.% I_2; (3) 0.25 vol.% I_2.

C_3H_6 yield (by 40–70%). Iodine promotes this oxidative dehydrogenation of propane by increasing both the propane conversion and propene selectivity. The selectivity increases to 93–97% at 400–450 °C. We found that the promoting effect of iodine did not depend on the method used for synthesis of VO_x/MgO samples and was about the same for all the catalysts studied by us. It is very important that iodine can be completely regenerated in this reaction. The sensitivity of our detection system was not sufficient to determine any iodinated products. Full iodine regeneration should make it possible to recover all iodine and use catalytically. So, the iodine-mediated oxidative dehydrogenation appears to be a very promising and rather general approach to improve the activity and selectivity in oxidative dehydrogenation of alkanes. We plan to study it in more detail later.

4. Conclusions

We have shown that mixed vanadium–magnesium hydroxide aerogels with the surface areas exceeding 1300 m^2/g can be synthesized by adjusting the aerogel synthesis conditions. Furthermore, the surface areas of such samples after calcination at high temperatures were substantially higher than those of the samples prepared by depositing vanadium precursor on MgO aerogels using other techniques. Comprehensive investigation of the synthesized catalysts by a number of physical methods proved that vanadium in these samples was stabilized in the forms of different partially crystalline or amorphous magnesium vanadates and vanadium dissolved in MgO rather than V_2O_5. The mixed aerogel method gave samples with the most uniform vanadium distribution that together with higher surface areas made these samples the most active VO_x/MgO catalysts in oxidative dehydrogenation of propane. Small amounts of iodine were shown to have a substantial favorable effect on the performance of all catalysts. As iodine can be successfully recovered, it can be considered to be an effective co-catalyst in this reaction that significantly improves both the catalyst selectivity and activity.

Acknowledgements

Financial support by the Russian Foundation for Basic Research (Grants 06-03-32712 and 06-03-32540) and the US Army Research Office is acknowledged with gratitude. The authors are grateful to CRDF (project RUE1-2893-NO-07) for financial support.

References

[1] P. Eisele, R. Killpack, Propene, Ullmanns Encyclopedia of Industrial Chemistry A22, VCH, Weinheim, 1993, 211.
[2] B. Frank, A. Dinse, O. Ovsitser, E.V. Kondratenko, R. Schomacker, Appl. Catal. A General 323 (2007) 66.
[3] J.F. Brazdil, Top. Catal. 38 (2006) 289.
[4] F. Cavani, N. Ballarini, A. Cericola, Catal. Today 127 (2007) 113.
[5] R. Ramos, M. Menendez, J. Santamaria, Catal. Today 56 (2000) 239.
[6] M.A. Chaar, D. Patel, M. Kung, H.H. Kung, J. Catal. 109 (1988) 463.
[7] D.S.H. Sam, V. Soenen, J.C. Volta, J. Catal. 123 (1990) 417.
[8] A. Corma, J.M. Lopez-Nieto, N. Paredes, Appl. Catal. A General 104 (1993) 161.
[9] E.A. Mamedov, V. Cortes Corberan, Appl. Catal. 127 (1995) 1.
[10] V. Soenen, J.M. Herrmann, J.C. Volta, J. Catal. 159 (1996) 410.
[11] D. Creaser, B. Andersson, Appl. Catal. A 141 (1996) 131.
[12] K. Chen, A. Khodakov, J. Yang, A.T. Bell, E. Iglesia, J. Catal. 186 (1999) 325.
[13] L. Late, E.A. Blekkan, J. Nat. Gas Chem. 11 (2002) 33.
[14] M. Sautel, G. Thomas, A. Kaddouri, C. Mazzocchia, R. Anouchinsky, Appl. Catal. A 155 (1997) 217.
[15] D.L. Stern, R.K. Grasselli, J. Catal. 167 (1997) 560.
[16] K. Chen, E. Iglesia, A.T. Bell, J. Phys. Chem. B 105 (2001) 646.
[17] P. Mars, D.W. van Krevelen, Chem. Eng. Sci. 3 (1954) 41.
[18] H.H. Kung, Adv. Catal. 1 (1994) 40.
[19] T. Blasco, J.M.L. Nieto, Appl. Catal. A 157 (1997) 117.
[20] S. Sugiyama, Y. Iozuka, E. Nitta, H. Hayashi, J.B. Moffat, J. Catal. 189 (2000) 233.
[21] M.M. Bettahar, G. Costentin, L. Savary, J.C. Lavalley, Appl. Catal. A 145 (1996) 1.
[22] J. Santamaria-Gonzalez, J. Luque-Zambrana, J. Merida-Robles, P. Maireles-Torres, E. Rodriguez-Casllon, A. Jimenez-Lopez, Catal. Lett. 68 (2000) 67.
[23] F. Arena, F. Frusteri, A. Parmaliana, G. Martra, S. Coluccia, Stud. Surf. Sci. Catal. 119 (1998) 665.
[24] Y.-M. Liu, Y. Cao, N. Yi, W.-L. Feng, W.-L. Dai, S.-R. Yan, H.-Y. He, K.-N. Fan, J. Catal. 224 (2004) 417.
[25] S. Utamapanya, K.J. Klabunde, J.R. Schlup, Chem. Mater. 3 (1991) 175.
[26] K.J. Klabunde, J.V. Stark, O.B. Koper, C. Mohs, D.G. Park, S. Decker, Y. Jiang, J. Lagadic, D. Zhang, J. Phys. Chem. 100 (1996) 12142.
[27] R. Richards, W. Li, S. Decker, C. Davidson, O. Koper, V. Zaikovskii, A. Volodin, T. Rieker, K.J. Klabunde, J. Am. Chem. Soc. 122 (2000) 4921.
[28] A.F. Bedilo, M.J. Sigel, O.B. Koper, M.S. Melgunov, K.J. Klabunde, J. Mater. Chem. 12 (2002) 3599.
[29] I.V. Mishakov, V.I. Zaikovskii, D.S. Heroux, A.F. Bedilo, V.V. Chesnokov, A.M. Volodin, I.N. Martyanov, S.V. Filimonova, V.N. Parmon, K.J. Klabunde, J. Phys. Chem. B 109 (2005) 6982.
[30] I.V. Mishakov, A.F. Bedilo, R.M. Richards, V.V. Chesnokov, A.M. Volodin, V.I. Zaikovskii, R.A. Buyanov, K.J. Klabunde, J. Catal. 206 (2002) 40.
[31] I.V. Mishakov, D.S. Heroux, V.V. Chesnokov, S.G. Koscheev, M.S. Mel'gunov, A.F. Bedilo, R.A. Buyanov, K.J. Klabunde, J. Catal. 229 (2005) 344.
[32] P.P. Gupta, K.L. Hohn, L.E. Erickson, K.J. Klabunde, A.F. Bedilo, AiChE. J. 50 (2004) 3195.
[33] C. Pak, A.T. Bell, T.D. Tilley, J. Catal. 206 (2002) 49.
[34] V.V. Chesnokov, A.F. Bedilo, D.S. Heroux, I.V. Mishakov, K.J. Klabunde, J. Catal. 218 (2003) 438.
[35] R. Vidal-Michel, K.L. Hohn, J. Catal. 221 (2004) 127.
[36] ICDD, PDF-2, 01-073-0207.
[37] ICDD, PDF-2, 00-036-0310.
[38] ICDD, PDF-2, 00-006-0767.
[39] ICDD, PDF-2, 00-045-0946.
[40] J.D. Pless, B.B. Bardin, H.-S. Kim, D. Ko, M.T. Smith, R.R. Hammond, P.C. Stair, K.R. Poeppelmeier, J. Catal. 223 (2004) 419.
[41] M. Anpo, S. Higashimoto, M. Matsuoka, N. Zhanpeisov, Y. Shioya, S. Dzwigaj, M. Che, Catal. Today 78 (2003) 211.
[42] M. Giorgetti, M. Berrettoni, S. Passerini, W.H. Smyrl, Electrochim. Acta 47 (2002) 3163.
[43] J. Wong, F.W. Lytle, R.P. Messmer, D.H. Maylotte, Phys. Rev. B 30 (1984) 5596.
[44] O. Sipr, A. Simunek, S. Bocharov, T. Kirchner, G. Drager, Phys. Rev. B 60 (1999) 14115.
[45] C. Pak, G.L. Hatter, Micropor. Mesopor. Mater. 44–45 (2001) 326.
[46] T. Tanaka, H. Yamashita, R. Tsuchitani, T. Funabiki, S. Yoshida, J. Chem. Soc., Faraday Trans. 84 (1988) 2987.
[47] M. Giorgetti, S. Passerini, W.H. Smyrl, S. Muckerjee, X.Q. Yang, J. McBreen, J. Eletrochem. Soc. 146 (1999) 2387.